OPEN ACCESS Freely available online

PLOS ONE

How Accurate Is MOLLI T1 Mapping In Vivo? Validation by Spin Echo Methods

Mitchell A. Cooper[1,2]*, Thanh D. Nguyen[2], Pascal Spincemaille[2], Martin R. Prince[2], Jonathan W. Weinsaft[2,3], Yi Wang[1,2]

1 Department of Biomedical Engineering, Cornell University, Ithaca, New York, United States of America, **2** Department of Radiology, Weill Cornell Medical College, New York, New York, United States of America, **3** Division of Cardiology, Department of Medicine, Weill Cornell Medical College, New York, New York, United States of America

Abstract

T_1 mapping is a promising quantitative tool for assessing diffuse cardiomyopathies. The purpose of this study is to quantify in vivo accuracy of the Modified Look-Locker Inversion Recovery (MOLLI) cardiac T_1 mapping sequence against the spin echo gold standard, which has not been done previously. T_1 accuracy of MOLLI was determined by comparing with the gold standard inversion recovery spin echo sequence in the calf muscle, and with a rapid inversion recovery fast spin echo sequence in the heart. T_1 values were obtained with both conventional MOLLI fitting and MOLLI fitting with inversion efficiency correction. In the calf (n = 6), conventional MOLLI fitting produced inconsistent T_1 values with error ranging from 8.0% at 90° to 17.3% at 30°. Modified MOLLI fitting with inversion efficiency correction improved error to under 7.4% at all flip angles. In the heart (n = 5), modified MOLLI fitting with inversion correction reduced T_1 error to 5.5% from 14.0% by conventional MOLLI fitting. This study shows that conventional MOLLI fitting can lead to significant in vivo T_1 errors when not accounting for the lower adiabatic inversion efficiency often experienced in vivo.

Citation: Cooper MA, Nguyen TD, Spincemaille P, Prince MR, Weinsaft JW, et al. (2014) How Accurate Is MOLLI T1 Mapping In Vivo? Validation by Spin Echo Methods. PLoS ONE 9(9): e107327. doi:10.1371/journal.pone.0107327

Editor: Xiaoliang Zhang, University of California San Francisco, United States of America

Received April 25, 2014; **Accepted** August 12, 2014; **Published** September 11, 2014

Data Availability: The authors confirm that, for approved reasons, some access restrictions apply to the data underlying the findings. De-identified data in this study is held in a research repository at Weill Cornell Medical College New York Presbyterian Hospital. Consenting volunteers to be a part of this repository is part of our HIPPA consent process. The consent allows for access of volunteer's data by outside researchers who promise in writing to keep the data private. Therefore this data cannot be made available to the general public. Data from this study can be requested from the repository by contacting Drs. Wang, Spincemaille, or Nguyen (authors on this study) directly, by contacting the Weill Cornell MRI Research Lab: http://weill.cornell.edu/mri/pages/about.html, or by contacting the Weill Cornell Radiology Department referencing this study: http://cornellradiology.com.

Funding: This research was supported in part by a National Science Foundation Graduate Research Fellowship (nsf.gov, DGE-0707428) and National Institutes of Health (nih.gov, grant HL064647). The funders had no role in study design, data collection and analysis, decision to publish, or preparation of the manuscript.

Competing Interests: YW is an academic editor for PLOS ONE. This does not alter the authors' adherence to PLOS ONE Editorial policies and criteria.

* Email: mac453@cornell.edu

Introduction

Myocardial T_1 mapping is a non-invasive MRI based tissue characterization technique that uses measurements of the T_1 relaxation time in the heart for diagnosis and treatment. T_1 mapping has been applied to a broad range of cardiac applications including quantification of lipid or iron deposition in the myocardium, and detection of subtle pathological changes due to edema [1]. In addition, T_1 mapping shows a great promise for assessing cardiac amyloidosis [2–4] and other non-ischemic or congenital cardiomyopathies that result in diffuse myocardial fibrosis [5–9]. The MOLLI (Modified Look Locker Inversion Recovery) sequence [10] is a fast 2D inversion recovery (IR) balanced steady-state free precession (bSSFP) based T_1 mapping method for cardiac imaging that is increasingly being used to probe differences between healthy and diseased states in the myocardium. While the accuracy of MOLLI has been studied extensively using computer simulations and water phantoms [10–13], a direct comparison of MOLLI with the gold standard IR spin echo (IR-SE) method has not yet been performed in vivo, where tissues may behave differently from water phantoms. This work aims to quantify MOLLI accuracy in vivo by comparing with the accurate but time-consuming gold standard IR-SE sequence in the calf muscle and with a rapid IR fast spin echo (IR-FSE) sequence in the heart of healthy volunteers. In addition, we quantified the effect of correcting for imperfect inversion efficiency [13–15] on the T_1 accuracy of MOLLI.

Materials and Methods

T_1 Fitting Approaches for MOLLI Data

The MOLLI sequence consists of inversion pulses followed by mixed periods of bSSFP readout and free relaxation and therefore has a fairly complex signal evolution (Fig.1). To overcome this problem, previous T_1 mapping studies using MOLLI typically approximated this signal curve using a mono-exponential fit to extract an apparent T1 relaxation time (T_1^*) and subsequently corrected it to yield an improved T_1 estimate [10]:

$$T_1 \approx T_1^* \left(\frac{B}{A} - 1 \right) \quad (1)$$

where T_1^* (the apparent T_1 relaxation), A and B are obtained by a three-parameter exponential fit of the MOLLI data (after restoring signal polarity and rearranging data according to their inversion times). While simple, this correction was originally derived for T_1

mapping with IR spoiled gradient echo (SPGR) Look-Locker imaging with continuous readouts [13,16] and therefore is not directly applicable to IR-bSSFP *modified* Look-Locker imaging with mixed readout and free relaxation periods. As a result, the correction in Eq.1 is known to deliver accurate T_1 estimates only for certain T_1/T_2 values and flip angles [11–13].

In addition to not fully accounting for complex MOLLI signal evolution (Fig.1), Eq.1 assumes perfect inversion efficiency (i.e., 100% of the longitudinal magnetization is inverted by the inversion pulse) [13–15]. Typically, long adiabatic inversion pulses (e.g., the hyperbolic secant pulse is approximately 8 ms on our system) are favored over short hard inversion pulses to provide uniform inversion in the presence of B_0 and B_1 field inhomogeneities in vivo [10,17]. These adiabatic pulses can introduce non-negligible T_2 induced signal loss in tissues with shorter T_2 relaxation times such as muscle and myocardium. It is possible to account for this error when the inversion efficiency is known. Reference [15] derived the following equation from Eq.1 to include inversion efficiency:

$$T_1 \approx T_1^* \left(\frac{B}{A} - 1 \right) \Big/ \delta \qquad (2)$$

where δ is the measured inversion efficiency. However, to our knowledge this has only been tested in phantoms [15] and has yet to be demonstrated in vivo. In this work, the inversion efficiency was obtained as a by-product of the T_1 fitting of the gold-standard IR-SE data and used in the fitting of MOLLI data.

Imaging Experiments

All experiments were performed on a 1.5T GE HDxt MRI scanner (GE Healthcare, Waukesha, WI) using an 8-channel receiver coil (GE Healthcare Coils, Aurora, OH). The study was approved by the Weill Cornell Institutional Review Board and all healthy volunteers provided written informed consent prior to imaging. Due to the length of the MRI study in the calf, healthy volunteers were enrolled in two separate groups for the calf and cardiac imaging experiments (one volunteer participated in both experiments). A 2D IR-SSFP MOLLI sequence was implemented following the method described in [10]. An 8.12 ms hyperbolic secant adiabatic inversion pulse and a 0.5 ms apodized half-sinc SSFP excitation pulse were used for all experiments.

MOLLI data was acquired in the calf muscle of 6 volunteers (5 men, 1 woman, mean age 30±6 years). Calf muscle was chosen for in vivo validation since its MR relaxation properties (T_1/T_2 ~1000/30 ms) are similar to that of myocardium (T_1/T_2 ~1100/50 ms). Imaging the calf muscle also eliminates the confounding effects of motion and heart rate variability on the T_1 accuracy of MOLLI [18,19], as well as enables the acquisition of the time-consuming gold standard IR-SE data, which is impractical in the heart. Typical MOLLI imaging parameters were as follows: TR = 4.1 ms, TE = 1.2 ms (asymmetric echo), matrix = 256×128 (interpolated to 256×256), FOV = 26–30 cm, partial FOV factor = 0.5, 11 inversion times (TI) = 100, 200, 350, 100+RR, 200+RR, 350+RR, 100+2RR, 200+2RR, 350+2RR, 350+3RR, 350+4RR (RR = cardiac interval). A 3 sec free relaxation period was introduced between subsequent modified Look-Locker experiments similar to that used in the original MOLLI sequence [10]. A 6 Kaiser-Bessel RF ramp [20] was used to prepare magnetization prior to SSFP data acquisition. MOLLI data were acquired with 30°, 60° and 90° readout flip angles. 2D IR-SE reference data was acquired with the following imaging parameters: TR = 6 sec, TE = 10 ms, matrix = 256×128 (interpolated to 256×256), partial FOV factor = 0.5, TI = 20, 300, 1000 ms and ∞, scan time = 26 min. Synthetic ECG gating signal (80 bpm) provided by the scanner software was used to avoid variations in the cardiac R-R interval.

Cardiac MOLLI data were acquired in 5 healthy volunteers (5 men, mean age 36±11 years) with peripheral gating and imaging parameters similar to that reported in [11,21]: TR = 3.3 ms, TE = 0.9 ms (asymmetric echo), flip angle = 30°, FOV = 35–36 cm, partial FOV factor = 0.75, parallel imaging (ASSET) factor R = 2, 11 TIs, 3 heartbeat pause between subsequent modified Look-Locker experiments, scan time = 17 heartbeats. Since the gold standard IR-SE sequence is too time-consuming for cardiac applications, a rapid cardiac gated single-shot IR-FSE sequence with variable refocusing flip angles was implemented to obtain reference myocardial T_1 within one breath-hold [22]. The typical IR-FSE imaging parameters were as follows: TR = 5 RR, minimum TE = 4 ms, echo train length = 48, matrix = 256×128, partial FOV factor = 0.75, TI = 20, 300, 1000 ms and ∞, ASSET factor R = 2, scan time = 16 heartbeats. Before use as a reference

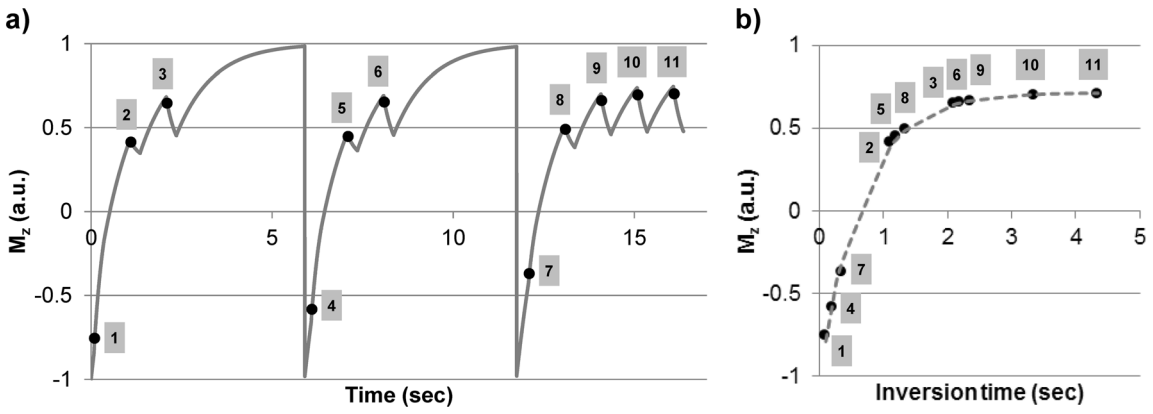

Figure 1. MOLLI acquisition and data fitting: a) Simulated longitudinal magnetization during MOLLI acquisition (T_1 = 1000 ms, T_2 = 30 ms, readout flip angle = 30°, echo train length = 64, heart rate = 60 bpm). Note the complex pattern of the underlying magnetization evolution due to mixed periods of bSSFP readout and free relaxation. MOLLI data are sampled at 11 inversion times marked; b) Conventional MOLLI fitting approximates the rearranged MOLLI data with a mono-exponential function to derive an apparent T_1, which is then corrected according to Eq.1.
doi:10.1371/journal.pone.0107327.g001

in the heart, the accuracy of the IR-FSE sequence was verified against the gold standard IR-SE in the calf muscle.

Data Analysis

All data were processed using Matlab R2009a (The Mathworks, Natick, MA) on a Dell XPS 8100 desktop computer. The polarity of the sampled data was restored using the method proposed in [23]. IR-SE data were fit using a three-parameter exponential signal equation $A - B \times \exp(-TI/T_1)$ to obtain the reference T_1 and inversion efficiency ($\delta = B/A - 1$). MOLLI data were fit using both conventional MOLLI fitting (Eq.1) and MOLLI fitting corrected with known inversion efficiency (Eq.2). Equation 2 used the inversion efficiency δ obtained from IR-SE acquisition.

In the calf, signals were averaged within a 3×3 region of interest (ROI) placed in the right soleus muscle of each volunteer prior to data fitting. There were no repeated measurements in the left and right calf muscles of the volunteers. For cardiac imaging, pixel-wise fitting was performed for an ROI placed in the left ventricular septum wall. IR-FSE data were processed using a three-parameter exponential fit to obtain the reference T_1.

Ideally one needs to perform mapping of inversion efficiency in the heart in order to accurately correct for myocardial T_1 obtained by MOLLI. Because this by itself is a difficult problem (e.g., due to respiratory and cardiac motion), a partial solution was pursued by mapping the inversion efficiency in the calf muscle and then adjusting this value for the heart muscle based on the theoretical difference predicted by Bloch simulation while accounting for expected values of T_1 and T_2 in the myocardium (see Results section).This allowed us to demonstrate the improved T_1 accuracy that can be obtained in the heart with inversion efficiency correction.

Relative T_1 error defined as $|T_{1,\mathrm{MOLLI}}-T_{1,\mathrm{IRSE}}|/T_{1,\mathrm{IRSE}} \times 100$ and relative fitting residual defined as $||S_{\mathrm{measured}}-S_{\mathrm{fitted}}||_2/||S_{\mathrm{measured}}||_2 \times 100$ were calculated, and statistical significance of the difference between the mean measured T_1 and the mean T_1 from IR-SE/FSE (gold standard) was determined using a one-way analysis of variance (ANOVA) followed by Tukey's post-hoc test for multiple comparison. A P-value of less than 0.05 was considered statistically significant.

Results

In the calf muscle (n = 6), conventional MOLLI fitting (Eq.1) produced fairly inaccurate and inconsistent T_1 values as the readout flip angle was varied, with average T_1 error reaching as high as 17.3% at 30° (Fig. 2a/Table 1). Interestingly, T_1 error by conventional MOLLI fitting was lower at higher flip angles (reducing to 8.0% at 90°) although the relative fitting residual increased markedly (Fig. 2b), from 3.7% at 30° (indicating a reasonable fit of the 3-parameter exponential model) to 11.8% at 90° (indicating a rather poor fit as shown in Fig. 2b/c). Using MOLLI fitting accounting for the inversion efficiency (Eq.2), error was improved to be less than 7.4% at all flip angles.

Figure 3 shows an example of T_1 maps obtained in the calf muscle at 30°. The average inversion efficiency g obtained from IR-SE and used in MOLLI data fitting was 85.7±1.6%. The average fitting time per pixel was 0.03 s for three-parameter MOLLI fitting, assuming that the polarity of the signal curve had already been restored.

In the calf muscle, the gold standard IR-SE and rapid IR-FSE acquisitions were found to provided similar T_1 values (1.3±0.7% relative error). However, the inversion efficiency measured by IR-FSE (81.9±2.0%) underestimated that obtained by IR-SE (85.7±1.6%) p = 0.002. To determine the in vivo inversion efficiency in the myocardium required for MOLLI data fitting, the theoretical inversion efficiency was simulated using T_1/T_2 of healthy soleus muscle (985/31 ms) [24] and myocardium (1088/52 ms) [22,25] and the shape of the adiabatic pulse used in the imaging experiment. Since simulation may not perfectly predict the in vivo inversion efficiency [15], the ratio of the simulated inversion efficiencies was then used to scale the average inversion efficiency obtained from the calf muscle (85.7%), yielding an inversion efficiency estimate of 88% for fitting of the cardiac data. B_1 and B_0 effects were not considered when estimating the inversion efficiency since the hyperbolic secant adiabatic inversion pulse is expected to be robust against B_1 and B_0 inhomogeneity encountered in vivo at 1.5 T. For T_1 and T_2 similar to that of the calf and the myocardium, the inversion efficiency is expected to vary by only a few percent with ± 25% variation in RF amplitude and ± 150 Hz off-resonance range as shown in Fig.4 of [15].

In the heart (n = 5), MOLLI with inversion correction (T_1 = 1065 ± 68 ms; p = 0.78) reduced T_1 error compared to conventional MOLLI fitting (T_1 = 937 ± 60 ms; p = 0.006) when compared to the reference T_1 values provided by IR-FSE (T_1 = 1092 ± 64 ms). Overall, the relative T_1 error was 14.0±6.6% for conventional MOLLI fitting, and 5.5±5.1% for MOLLI with inversion efficiency correction, closely following the trend observed in the calf experiments. A comparison of short-axis myocardial T_1 maps obtained with the two MOLLI data fitting methods is shown in Fig.4. The average heart rate was 52.8±9.6 bpm (range 40–63 bpm).

Discussion

Our in vivo data showed that conventional MOLLI (Eq.1) provided fairly inaccurate and inconsistent in vivo T_1 values in muscle tissues when compared with the standard spin echo based methods. As indicated by our results, a major source of T_1 error comes from reduced adiabatic inversion efficiency due to shorter T_2 of muscle tissues (T1/T2 ratio ~30). The correction for apparent T_1 used in the conventional MOLLI fitting was originally derived for SPGR Look-Locker imaging assuming 100% inversion efficiency and therefore may not be adequate for describing a more complicated bSSFP signal evolution in MOLLI (Fig.1), especially at reduced inversion efficiency. Limitations of the model are shown in figure 2 when imaging at higher flip angles causes larger fitting residuals. When accounting for the inversion efficiency in conventional MOLLI fitting (Eq. 2), T_1 error was greatly reduced. The current work shows that conventional fitting after inversion efficiency correction (Eq. 2) is valid, even though, strictly speaking, it only applies to spoiled gradient echo based Look-Locker acquisitions [13,16]. This finding agrees well with recent results obtained with an SPGR based MOLLI sequence at 7T [14] and serves to confirm that a source of error with traditional MOLLI T1 mapping is the inversion efficiency, which can be improved upon when using Eq. 2 if the inversion efficiency is measured. Further in vivo studies may be warranted to quantify T_1 error in MOLLI as a function of inversion efficiency in different tissues.

The conventional MOLLI fitting method (Eq.1) has been validated in water phantoms doped with various contrast agents [10–12,18] by comparing with the gold standard IR-SE method. However, water phantoms are different from in vivo tissue in biochemical composition and underlying biophysical process (e.g., exchange among water compartments), resulting in different relaxation and MRI signal behavior. In vivo validation of MOLLI has not been performed so far most likely due to the excessive IR-SE acquisition time. In this work, we used the calf muscle as a

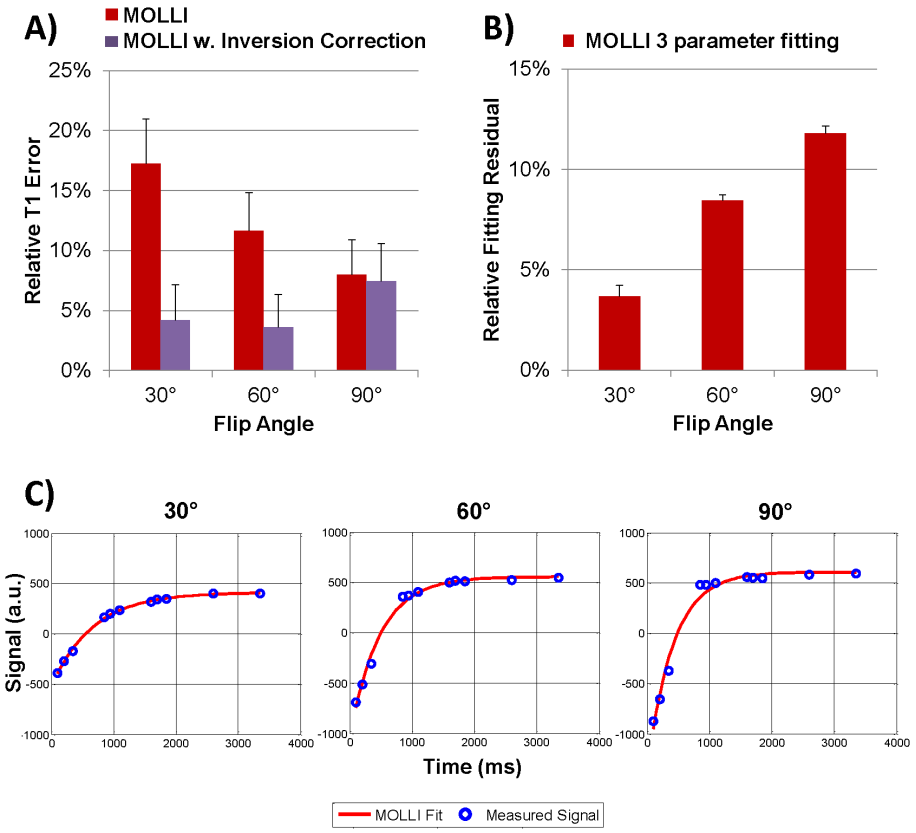

Figure 2. MOLLI results in the calf muscle (n = 6): A) T_1 errors obtained at 30°, 60° and 90° readout flip angle for conventional MOLLI fitting (Eq.1) and MOLLI fitting with inversion correction (Eq.2); B) Relative fitting residuals for the three parameter fit used in Eqs.1 and 2. Note the increasing residuals with the three parameter fitting (used by Eqs.1 and 2) at higher flip angles; C) Measured signal and curves fit with the 3-parameter MOLLI fit in the calf muscle of one volunteer at 30°, 60° and 90°. Notice the increasing discrepancy between the fit and measured data at higher flip angle, confirmed by the increase in fitting residual in (B).
doi:10.1371/journal.pone.0107327.g002

Table 1. Comparison of T1 values obtained in the calf muscle (n = 6) and myocardium (n = 5) of healthy volunteers using conventional MOLLI fitting (Eq.1) and MOLLI fitting with inversion correction (Eq.2) at various flip angles (FA).

Calf Muscle (n = 6)

			FA = 30°		FA = 60°		FA = 90°	
	IR-SE	IR-FSE	MOLLI	MOLLI w. Inv	MOLLI	MOLLI w. Inv	MOLLI	MOLLI w. INV
T1 (ms)	986±32	987±42	815±40	952±38	871±36	1016±27	907±35	1058±27
Inv. Eff.	85.7±1.6%	81.9±2.0%	N/A					
P	N/A	1	<0.001	0.69	<0.001	0.79	0.007	0.02
Fitting residual			3.7±0.6%		8.5±0.3%		11.8±0.36%	

Myocardium (n = 5)

		FA = 30°	
	IR-FSE	MOLLI	MOLLI w. Inv
T1 (ms)	1092±64	937±60	1065±68
Inv. Eff.	88% (sim. from calf and Bloch)	N/A	
P	N/A	0.006	0.78
Fitting residual		5.3%±1.8%	

P values are given for comparison with the gold standard IR-SE method (calf) or IR-FSE method (myocardium).
doi:10.1371/journal.pone.0107327.t001

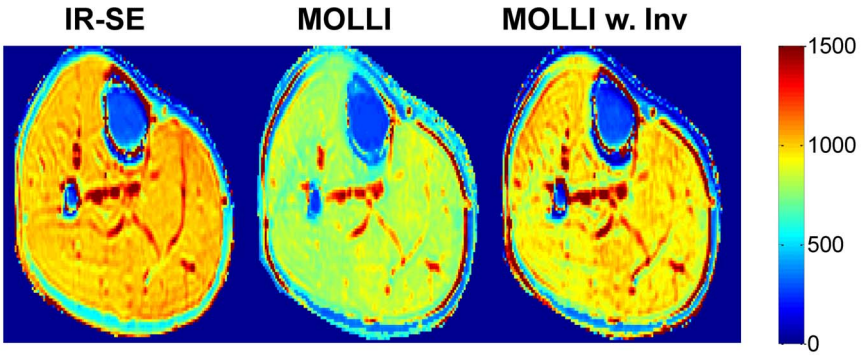

Figure 3. Example of T_1 maps (in ms) obtained with IR-SE, conventional MOLLI fitting and MOLLI fitting with inversion correction in the calf muscle at 30° flip angle.
doi:10.1371/journal.pone.0107327.g003

tissue model for the myocardium, thus enabling for the first time a direct in vivo comparison of MOLLI with IR-SE. For cardiac T_1 mapping, a more rapid IR-FSE sequence was developed to enable cardiac T_1 mapping in a single breath-hold [22]. While conventional MOLLI fitting of phantom data traditionally shows good to excellent T_1 accuracy [10–12,18], we found larger in vivo T_1 errors (above 10%) in both the calf muscle and the myocardium which could be reduced to less than 7.4% when accounting for inversion efficiency as in Eq.2. This observation suggests that in vivo validation should be considered following the initial phantom validation when assessing the performance of T_1 mapping for in vivo imaging.

Our in vivo T_1 results obtained with the conventional MOLLI fitting (Eq.1) are similar to that reported in previous studies (761 ms in the skeletal muscle [10] and 962–998 ms in the myocardium [10,18,21]). Interestingly, we observed increasing T_1 values at higher readout flip angles in the calf muscle, a trend opposite to that reported previously in the myocardium [11]. To better understand this phenomenon, we have performed Bloch simulation for T_1/T_2 of the calf muscle and the heart and observed that the trend highly depends on tissue T_2 and other timing parameters such as heart rate. In addition, conventional MOLLI analysis (Eq.1) does not explicitly take into account the flip angle, since it was originally derived for SPGR imaging, and as a result can provide a flip angle dependent bias specific to tissue T1/T2. This bias may explain the increase in T1 error after inversion efficiency correction, especially at higher flip angles of 60° and 90°. This is additional evidence that the conventional MOLLI data fitting may not work well for different tissues or when imaging conditions are changed.

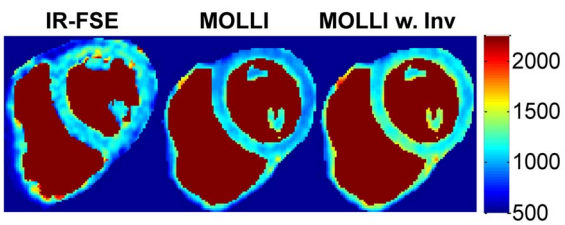

Figure 4. Example of myocardial T_1 maps (in ms) obtained with IR-FSE, conventional MOLLI fitting and MOLLI fitting with inversion correction at a 30° flip angle. The IR-FSE image was taken in a separate breath-hold than the MOLLI and therefore it is at a slightly different position. Blood has been segmented out to minimize distraction due to the blood T_1: IR-FSE spoils the blood signal and is not able to fit for blood T_1, however MOLLI is able to fit for T_1 in the blood.
doi:10.1371/journal.pone.0107327.g004

The above findings are clinically relevant for two reasons. First, inversion efficiency correction can significantly reduce T_1 error in MOLLI to within 7.4%, thereby improving the reliability of this technique for diagnostic purposes. Second, the improved consistency of T_1 estimates at different flip angles and T_1/T_2 values after applying correction (Eq. 2) to MOLLI analysis may benefit multi-site multi-vendor T_1 mapping studies by reducing discrepancies due to different hardware and software implementations.

This work has several limitations. The effect of inversion efficiency on T_1 fitting post contrast, which is important for clinical application, was not investigated. This was because myocardial T_1 can vary significantly post contrast depending on factors such as cardiac output and bolus timing, making accurate comparisons between the reference IR-FSE sequence and the MOLLI sequence in multiple subjects challenging. The long echo train of the IR-FSE sequence may also result in errors due to blurring in tissue with short T_1. The trade-off between scan time reduction by prolonging the echo train (which is relevant for breath-hold cardiac imaging) and the associated image blurring in such situations is an important question and will be investigated in our future work. In addition, post-contrast myocardial T_2 is difficult to measure for the same reason, making the estimation of inversion efficiency non-trivial. In this work, in vivo inversion efficiency was obtained as a by-product of IR-SE data fitting, which is not a practical method due to long IR-SE acquisition time and the lack of experimental mapping of in vivo inversion efficiency in the heart further limited the work.

A fitting method that can improve MOLLI T1 estimates in vivo using Eq.2 would require the knowledge of imaging and tissue parameters (e.g., inversion efficiency), which may not be readily available. Mapping inversion efficiency, for example, is a non-trivial problem particularly in the in vivo setting, and this is an important limitation of the MOLLI approach. Another possible avenue for inversion efficiency correction in MOLLI would be to measure the inversion efficiency in the calf in an initial study in both healthy subjects and patients, and then establish and validate a population average. We believe however that IR-FSE is a better approach in patients with lower heart rate (to reduce the motion sensitivity of the FSE readout) and when blood T_1 is not needed. Another potential solution could be to fit for the inversion efficiency, however this requires the use of an SPGR readout with reduced SNR efficiency a four parameter fit that is more sensitive to noise [14]. A shorter adiabatic pulse could also be used to

improve the inversion efficiency, although this is often limited by the maximum allowable RF transmit power [15].

Other potential factors limiting MOLLI accuracy in vivo, but not studied here, were reviewed in [13] and may include, but are not limited to deviation from the nominal flip angle profile [24,26], heart rate variability [18,27,28], magnetization transfer (MT) effect [26,29–31], motion [19], and B_0 inhomogeneity [13,32]. Recent works have proposed acquiring MT sensitive data (e.g., by varying RF pulse length) and including MT effect in the signal model [26,29,30] for accurate T_1 fitting; however, the utility of this approach for cardiac T_1 mapping using MOLLI remains to be investigated. A potential solution for these imperfections could be to develop a IR-FSE based T_1 mapping sequence [22] which is more robust against imperfect inversion efficiency and field inhomogeneities than the bSSFP based MOLLI sequence.

In conclusion, the conventional correction (Eq.1) of apparent T_1 in MOLLI can lead to significant in vivo T_1 errors partly due to lower adiabatic inversion efficiency in muscle tissues. T_1 errors can be reduced significantly by using a modified version of the conventional MOLLI correction accounting for inversion efficiency (Eq.2), when the inversion efficiency is known.

Author Contributions

Conceived and designed the experiments: MAC TDN JWW. Performed the experiments: MAC TDN. Analyzed the data: MAC TDN PS YW MRP. Contributed reagents/materials/analysis tools: MAC TDN. Contributed to the writing of the manuscript: MAC TDN PS MRP JWW YW.

References

1. Moon JC, Messroghli DR, Kellman P, Piechnik SK, Robson MD, et al. (2013) Myocardial T1 mapping and extracellular volume quantification: a Society for Cardiovascular Magnetic Resonance (SCMR) and CMR Working Group of the European Society of Cardiology consensus statement. J Cardiovasc Magn Reson 15: 92.
2. Maceira AM, Joshi J, Prasad SK, Moon JC, Perugini E, et al. (2005) Cardiovascular magnetic resonance in cardiac amyloidosis. Circulation 111: 186–193.
3. Maceira AM, Prasad SK, Hawkins PN, Roughton M, Pennell DJ (2008) Cardiovascular magnetic resonance and prognosis in cardiac amyloidosis. J Cardiovasc Magn Reson 10: 54.
4. Krombach GA, Hahn C, Tomars M, Buecker A, Grawe A, et al. (2007) Cardiac amyloidosis: MR imaging findings and T1 quantification, comparison with control subjects. J Magn Reson Imaging 25: 1283–1287.
5. Sparrow P, Messroghli DR, Reid S, Ridgway JP, Bainbridge G, et al. (2006) Myocardial T1 mapping for detection of left ventricular myocardial fibrosis in chronic aortic regurgitation: pilot study. AJR Am J Roentgenol 187: W630–635.
6. Iles L, Pfluger H, Phrommintikul A, Cherayath J, Aksit P, et al. (2008) Evaluation of diffuse myocardial fibrosis in heart failure with cardiac magnetic resonance contrast-enhanced T1 mapping. J Am Coll Cardiol 52: 1574–1580.
7. Sibley CT, Noureldin RA, Gai N, Nacif MS, Liu S, et al. (2012) T1 Mapping in cardiomyopathy at cardiac MR: comparison with endomyocardial biopsy. Radiology 265: 724–732.
8. Lu M, Zhao S, Yin G, Jiang S, Zhao T, et al. (2013) T1 mapping for detection of left ventricular myocardial fibrosis in hypertrophic cardiomyopathy: a preliminary study. Eur J Radiol 82: e225–231.
9. Broberg CS, Chugh SS, Conklin C, Sahn DJ, Jerosch-Herold M (2010) Quantification of diffuse myocardial fibrosis and its association with myocardial dysfunction in congenital heart disease. Circ Cardiovasc Imaging 3: 727–734.
10. Messroghli DR, Radjenovic A, Kozerke S, Higgins DM, Sivananthan MU, et al. (2004) Modified Look-Locker inversion recovery (MOLLI) for high-resolution T1 mapping of the heart. Magn Reson Med 52: 141–146.
11. Messroghli DR, Greiser A, Frohlich M, Dietz R, Schulz-Menger J (2007) Optimization and validation of a fully-integrated pulse sequence for modified look-locker inversion-recovery (MOLLI) T1 mapping of the heart. J Magn Reson Imaging 26: 1081–1086.
12. Gai ND, Stehning C, Nacif M, Bluemke DA (2013) Modified Look-Locker T1 evaluation using Bloch simulations: Human and phantom validation. Magnetic Resonance in Medicine 69: 329–336.
13. Kellman P, Hansen M (2014 Jan 4; doi: 10.1186/1532-429X-16-2 [Epub ahead of print].) T1-mapping in the heart: accuracy and precision. Journal of Cardiovascular Magnetic Resonance.
14. Rodgers CT, Piechnik SK, Delabarre LJ, Van de Moortele PF, Snyder CJ, et al. (2012) Inversion recovery at 7 T in the human myocardium: Measurement of T(1), inversion efficiency and B(1) (+). Magn Reson Med.
15. Kellman P, Herzka DA, Hansen MS (2014) Adiabatic inversion pulses for myocardial T1 mapping. Magn Reson Med 71: 1428–1434.
16. Deichmann R, Haase A (1992) Quantification of T1 values by SNAPSHOT-FLASH NMR imaging. Journal of Magnetic Resonance (1969) 96: 608–612.
17. Kim D, Cernicanu A, Axel L (2005) B(0) and B(1)-insensitive uniform T(1)-weighting for quantitative, first-pass myocardial perfusion magnetic resonance imaging. Magn Reson Med 54: 1423–1429.
18. Piechnik SK, Ferreira VM, Dall'Armellina E, Cochlin LE, Greiser A, et al. (2010) Shortened Modified Look-Locker Inversion recovery (ShMOLLI) for clinical myocardial T1-mapping at 1.5 and 3 T within a 9 heartbeat breathhold. J Cardiovasc Magn Reson 12: 69.
19. Xue H, Shah S, Greiser A, Guetter C, Littmann A, et al. (2012) Motion correction for myocardial T1 mapping using image registration with synthetic image estimation. Magn Reson Med 67: 1644–1655.
20. Nguyen TD, Spincemaille P, Prince MR, Wang Y (2006) Cardiac fat navigator-gated steady-state free precession 3D magnetic resonance angiography of coronary arteries. Magn Reson Med 56: 210–215.
21. Messroghli DR, Plein S, Higgins DM, Walters K, Jones TR, et al. (2006) Human myocardium: single-breath-hold MR T1 mapping with high spatial resolution—reproducibility study. Radiology 238: 1004–1012.
22. Nguyen TD, Cooper MA, Spincemaille P, Weinsaft JW, Prince MR, Wang Y. A new method for accurate myocardial T1 mapping using Variable Angle Long Echo train Relaxometric Imaging (VALERI). Proceedings of the 21st Annual Meeting ISMRM; 2013; Salt Lake City, UT. pp. 262.
23. Nekolla S, Gneiting T, Syha J, Deichmann R, Haase A (1992) T1 maps by K-space reduced snapshot-FLASH MRI. J Comput Assist Tomogr 16: 327–332.
24. Cooper MA, Nguyen TD, Spincemaille P, Prince MR, Weinsaft JW, et al. (2012) Flip angle profile correction for T(1) and T(2) quantification with look-locker inversion recovery 2D steady-state free precession imaging. Magn Reson Med 68: 1579–1585.
25. Giri S, Chung YC, Merchant A, Mihai G, Rajagopalan S, et al. (2009) T2 quantification for improved detection of myocardial edema. J Cardiovasc Magn Reson 11: 56.
26. Ehses P, Seiberlich N, Ma D, Breuer FA, Jakob PM, et al. (2013) IR TrueFISP with a golden-ratio-based radial readout: fast quantification of T1, T2, and proton density. Magn Reson Med 69: 71–81.
27. Fitts M, Breton E, Kholmovski EG, Dosdall DJ, Vijayakumar S, et al. (2013) Arrhythmia insensitive rapid cardiac T1 mapping pulse sequence. Magn Reson Med 70: 1274–1282.
28. Weingartner S, Akcakaya M, Basha T, Kissinger KV, Goddu B, et al. (2013) Combined saturation/inversion recovery sequences for improved evaluation of scar and diffuse fibrosis in patients with arrhythmia or heart rate variability. Magn Reson Med.
29. Gloor M, Scheffler K, Bieri O (2008) Quantitative magnetization transfer imaging using balanced SSFP. Magn Reson Med 60: 691–700.
30. Gloor M, Scheffler K, Bieri O. Analytical description of magnetization transfer effects on the transient phase of balanced SSFP. Proceedings of the 20th Annual Meeting ISMRM; 2012; Melbourne, Australia. pp. 4262.
31. Robson MD, Piechnik SK, Tunnicliffe EM, Neubauer S (2013) T measurements in the human myocardium: The effects of magnetization transfer on the SASHA and MOLLI sequences. Magn Reson Med.
32. Kellman P, Herzka DA, Arai AE, Hansen MS (2013) Influence of Off-resonance in myocardial T1-mapping using SSFP based MOLLI method. J Cardiovasc Magn Reson 15: 63.